Journal of Viral Hepatitis, 2009 doi:10.1111/j.1365-2893.2009.01221.x

Hepatitis A virus (HAV) proteinase 3C inhibits HAV IRES-dependent translation and cleaves the polypyrimidine tract-binding protein

T. Kanda,[1] V. Gauss-Müller,[2] S. Cordes,[2] R. Tamura,[1] K. Okitsu,[1] W. Shuang,[1] S. Nakamoto,[1] K. Fujiwara,[1] F. Imazeki[1] and O. Yokosuka[1] [1]*Department of Medicine and Clinical Oncology, Graduate School of Medicine, Chiba University, Inohana, Chuo-ku, Chiba, Japan; and* [2]*Institute of Medical Molecular Biology, University of Lübeck, Lübeck, Germany*

Received July 2009; accepted for publication September 2009

SUMMARY. Hepatitis A virus (HAV) infection is still an important issue worldwide. A distinct set of viruses encode proteins that enhance viral cap-independent translation initiation driven by an internal ribosome entry site (IRES) and suppress cap-dependent host translation. Unlike cytolytic picornaviruses, replication of HAV does not cause host cell shut off, and it has been questioned whether HAV proteins interfere with its own and/or host translation. HAV proteins were coexpressed in Huh-7 cells with reporter genes whose translation was initiated by either cap-dependent or cap-independent mechanisms. Among the proteins tested, HAV proteinase 3C suppressed viral IRES-dependent translation. Furthermore, 3C cleaved the polypyrimidine tract-binding protein (PTB) whose interaction with the HAV IRES had been demonstrated previously. The combined results suggest that 3C-mediated cleavage of PTB might be involved in down-regulation of viral translation to give way to subsequent viral genome replication.

Keywords: 3C protease, hepatitis A virus, IRES, PTB, translation.

INTRODUCTION

The messenger-sense RNA genome of hepatitis A virus (HAV) is about 7500 nucleotides in length and contains a single large open-reading frame (ORF) encoding a polyprotein with the capsid proteins representing the amino-terminal third and the remainder comprising a series of nonstructural proteins required for viral RNA replication: 2B, 2C, 3A, 3B, $3C^{pro}$ (cysteine proteinase responsible for most post-translational cleavage events within the polyprotein) and $3D^{pol}$ (RNA-dependent RNA polymerase, see Fig. 1a, top panel) [1]. In a regulated cascade, the viral polyprotein is cleaved by $3C^{pro}$ into intermediate and mature products that fulfill distinct functions in the viral life cycle. At both ends of the picornaviral genome, the ORF is flanked by highly structured nontranslated regions (5′NTR and 3′NTR). The down-stream part of the 5′NTR presents an internal ribosome entry site (IRES) that allows translation by a cap-independent mechanism [1–3]. Several IRES trans-acting factors (ITAF) have been identified as mediating IRES binding to the ribosome [4]. Whereas glyceraldehyde-3-phosphate-dehydrogenase (GAPDH) and La autoantigen suppress HAV IRES activity, the poly(C)-binding protein (PCBP) and the polypyrimidine tract-binding protein (PTB) were found to enhance HAV translation [3,5–9]. PTB, a 57-kDa protein, is a member of the heterogeneous nuclear ribonucleoprotein family that shuttles between the nucleus and cytoplasm [10]. While experimental data have demonstrated PTB binding to polypyrimidine tracts (UCUUU or UCUUC) in picornaviral IRES, the exact cellular functions of PTB are as yet incompletely defined [3,10,11].

Proteolytic cleavage of host proteins is a common mechanism executed by picornaviruses to shut off host cell protein synthesis and to regulate viral protein and RNA synthesis. These two synthetic processes are central in the viral life cycle and mutually exclusive on the same RNA template. As HAV does not shut off host protein synthesis, it seems that HAV cap-independent translation constantly

Abbreviations: GAPDH, glyceraldehyde-3-phosphate-dehydrogenase; HAV, Hepatitis A virus; IRES, internal ribosome entry site; ITAF, IRES trans-acting factors; ORF, open-reading frame; PABP, poly(A)-binding protein; PCBP, poly(C)-binding protein; PTB, polypyrimidine tract-binding protein.

Correspondence: Dr Tatsuo Kanda, Department of Medicine and Clinical Oncology, Graduate School of Medicine, Chiba University, 1-8-1 Inohana, Chuo-ku, Chiba 260-8677, Japan. E-mail: kandat-cib@umin.ac.jp

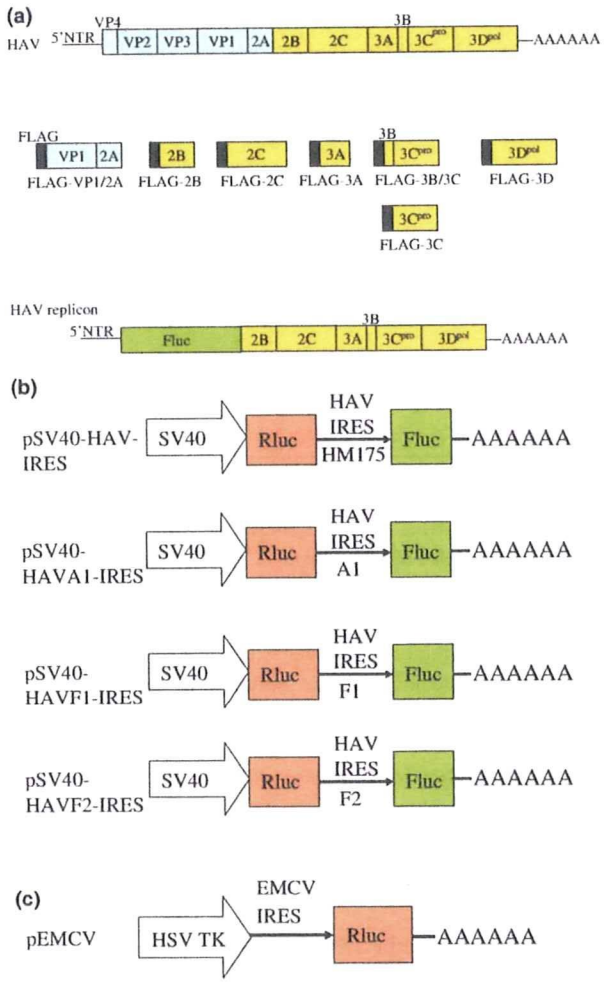

Fig. 1 Schematic representation of the hepatitis A virus (HAV) constructs used in this study. (a) Structures of the HAV genome (upper panel), FLAG-tagged HAV proteins (middle panel; ref. 17) and HAV replicon pT7-18f-luciferase (lower panel; ref. 13). AAAAAA, poly A tail. (b) Structure of the bicistronic plasmids used. pSV40-HAV-internal ribosome entry site (IRES) encodes the Renilla luciferase, the IRES of HAV strain HM175 and the firefly luciferase (Fluc) under the control of the simian virus 40 promoter (SV40) (ref. 16). pSV40-HAVA1-IRES, pSV40-HAVF1-IRES and pSV40-HAVF2-IRES encode IRES elements derived from an acute hepatitis and two fulminant hepatitis cases, respectively. (c) Structure of plasmid pEMCV.

competes with cap-dependent translation of host proteins [1,12]. In this study, we show that HAV $3C^{pro}$ cleaved PTB and suppressed cap-independent translation initiation. The data indicate that the viral proteinase might play an important role in the regulation of HAV IRES-mediated cap-independent translation by targeting noncanonical translation factors.

MATERIALS AND METHODS

Cell lines

Huh-7, a human hepatoma cell line, and its stably transformed derivative Huh-T7 that expresses the T7 RNA polymerase [3] were grown in Dulbecco's modified Eagle medium (Gibco BRL, Gaithersburg, MD, USA) supplemented with 10% heat-inactivated foetal bovine serum with or without G418 sulfate (400 μg/mL; Promega, Madison, WI, USA), in addition to penicillin and streptomycin.

Plasmids

pT7-18f-luciferase (LUC), a replication-competent HAV replicon, containing an open-reading frame with the firefly luciferase (Fluc) flanked by the first four amino acids of the HAV polyprotein and by 12 C-terminal amino acids of VP1, followed by the P2 and P3 domains of the HAV polyprotein (HAV strain HM175 18f, GenBank Accession No. M59808), and pT7-18f-LUCmut, a replication-deficient replicon, were described previously [13] (Fig. 1a).

The constructs encoding the simian virus 40 (SV40) promoter-driven *Renilla reniformis* luciferase (Rluc), the IRES derived from the cell culture adapted HAV strain HM175 [14], and Fluc, named pSV40-HAV-IRES, was prepared as described previously [2,15] (Fig. 1b). To investigate the specific effect exerted by the HAV IRES sequences, bicistronic reporter constructs (pSV40-HAVA1-IRES, pSV40-HAVF1-IRES and pSV40-HAVF2-IRES; Kanda *et al.*, manuscript in preparation) were prepared, which included the IRES of clinical specimens. Construction of HAV protein expression plasmids was described previously [16]. Briefly, seven regions of the HAV genome were amplified by reverse transcription-polymerase chain reaction (PCR) with HAV region-specific primers [16]. These regions were HAV VP1-2A, 2B, 2C, 3A, 3BC, 3C and 3D. The amplified products were cloned into pCXN2 (kindly provided by Prof. J. Miyazaki, Osaka University, Japan), a mammalian expression vector with a beta-actin-based CAG promoter and a SV40 origin [17], to generate pCXN2-FLAG-VP1-2A, 2B, 2C, 3A, 3BC, 3C, 3D expressing FLAG-tagged proteins [16] (Fig. 1a). To control for the target specificity, pEMCV, which contains the encephalomyocarditis virus (EMCV) IRES upstream of Rluc, was generated (Fig. 1c). Transient expression of $3C^{pro}$ using vaccinia virus, pGEM-3C, and pEXT7-HAV3C was described before [12].

Transfection and protein analyses

Approximately 60% confluent Huh-7 cells, grown in 6-well culture plates, were transfected with 0.3 μg of the LUC reporter plasmid and 0.1 μg of each HAV protein-expressing plasmid using Effectene transfection reagent (Qiagen, Tokyo, Japan). Forty-eight hours after transfection, cell

extracts were prepared, and a LUC assay kit (Toyo Ink, Tokyo, Japan) was used according to the manufacturer's instructions. LUC activity was measured in relative light units with a luminometer (AB-2200-R; ATTO, Tokyo, Japan). The assays were adjusted to protein amount and were conducted, on average, in duplicate [18]. To determine cleavage of the host proteins PTB and poly(A)-binding protein (PABP), extracts of transfected cells were analysed for viral antigen and host proteins, as described previously [12]. Viral proteins were identified using anti-FLAG and anti-HAV 3C antibodies. PTB was recognized by the monoclonal antibody BB7 [19].

RESULTS

HAV proteinases 3BC and 3C suppress IRES-dependent translation

Translation of the HAV polyprotein is initiated cap-independently and is driven by an IRES. As a first approach to assess the role of HAV proteins, we examined cap-independent and cap-dependent translation using the bicistronic reporter constructs depicted in Fig. 1. pSV40-HAV-IRES, which contains the IRES of HAV strain HM175 (Fig. 1b), was transfected into Huh-7 together with various expression vectors encoding FLAG-tagged HAV protein (Fig. 1a). The expression of these proteins was confirmed by Western blotting with anti-FLAG antibodies (data not shown and ref. 16). Compared to the control (pCXN2) and to the other HAV proteins tested (VP1-2A, 2B, 2C, 3A and 3D), expression of HAV 3BC or 3C specifically inhibited cap-independent translation initiated by the HAV IRES as determined by the Fluc activity (Fig. 2).

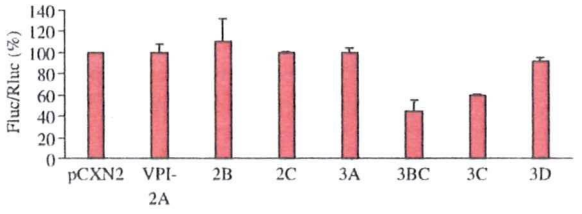

Fig. 2 Effects of hepatitis A virus (HAV) proteins on HAV internal ribosome entry site (IRES)-dependent translation. Relative luciferase activities are indicated (IRES/Cap; firefly luciferase/*Renilla reniformis* luciferase, %). Luciferase activities were determined in three independent experiments. Error bars represent standard errors of the mean.

To corroborate the observed suppression of HAV IRES-independent translation, we next examined the effect of $3C^{pro}$ on translation, which was dependent on HAV IRES elements derived from clinical isolates; IRES A1 was taken from an acute self-limited hepatitis (pSV40-HAVA1-IRES), and F1 and F2 were derived from fulminant HAV infections (pSV40-HAVF1-IRES and pSV40-HAVF2-IRES) (Fig. 3a–c). After coexpression of pSV40-HAVA1-IRES, pSV40-HAVF1-IRES and pSV40-HAVF2-IRES with 3BC or $3C^{pro}$, the Fluc activity was specifically suppressed when compared to the control (pCXN2, Fig. 3a–c). The results confirm our findings shown in Fig. 2 and demonstrate that HAV proteinases 3BC and $3C^{pro}$ suppress HAV IRES-dependent translation. For yet unknown reasons, the negative effect of 3BC was generally more pronounced than that exerted by $3C^{pro}$. However, as $3C^{pro}$ is the prevailing and stable form of the viral proteinase, only this form was used in the subsequent studies.

Translation of the viral polyprotein is the first metabolic step in the viral life cycle and a prerequisite for viral RNA synthesis. It can be assumed that a negative effect on

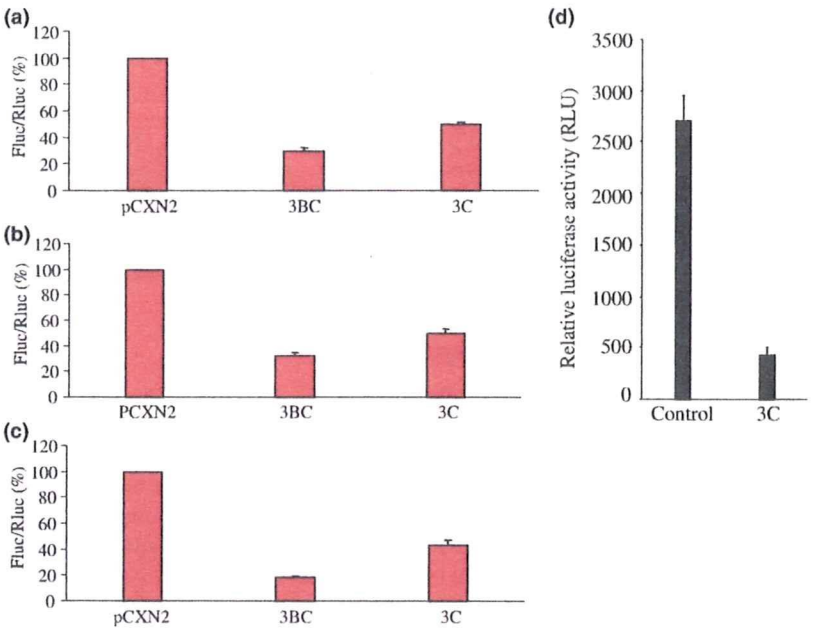

Fig. 3 Effects of hepatitis A virus (HAV) 3BC or $3C^{pro}$ on HAV internal ribosome entry site (IRES)-dependent translation (a–c) and on expression of the HAV replicon [pT7-18f-luciferase (LUC)] (d). HAV was derived from clinical isolates: (a) acute hepatitis; (b) and (c) two forms of fulminant hepatitis. Relative luciferase activities are indicated (IRES/Cap; firefly luciferase/*Renilla reniformis* luciferase, %) (a–c). LUC activities are presented as an average of three independent experiments. Error bars represent standard errors of the mean. RLU, relative light units.

translation might indirectly cause a reduction in viral genome production. HAV replication was efficiently studied using the viral replicon (see Fig. 1a, lower panel) with Fluc as reporter gene in place of the viral structural proteins [13]. The reporter gene activity is directly proportional to viral RNA synthesis. To investigate whether 3C-mediated suppression of translation affects genome replication, we cotransfected HAV replicon RNA with the 3C-expression or control vector into Huh-T7 cells (Fig. 3d). HAV replicon replication was monitored by reporter assay 72 h post-transfection. Compared to the replication-deficient replicon (pT7-18f-LUCmut), the reporter activity at this point was derived from newly synthesized viral genomes and therefore represents viral genome synthesis [13]. Compared to the control, HAV replication was significantly suppressed in the presence of excess 3C, indicating that 3C-mediated inhibition of translation restrained HAV genome replication in human hepatoma cells.

To assess the specificity of the inhibitory effect exerted by HAV proteinase $3C^{pro}$, translation initiated at the EMCV IRES was compared with the HAV IRES. For this, HAV $3C^{pro}$ was coexpressed with pEMCV (Fig. 1c), and the Rluc activity of the cell extracts collected 48 h post-transfection was determined. Compared to the HAV IRES tested in parallel experiments, the EMCV IRES activity was similar in the presence and absence of coexpressed HAV $3C^{pro}$ [118 ± 29 (%)]. Combined and in light of the results described in the following, these findings suggest that an essential ITAF was cleaved by HAV $3C^{pro}$. As shown in the following, HAV $3C^{pro}$ partially cleaved PTB, whose active role in picornaviral IRES-dependent translation has been demonstrated previously [6,8]. As EMCV IRES translation was unaffected by HAV $3C^{pro}$, PTB is not an essential ITAF for this IRES, confirming an earlier report [20]. Intriguingly, an excess of PTB even suppressed EMCV IRES-driven translation [21]. The abundance and distribution of PTB varies significantly among cell types [6,8]. Large amounts of PTB were found in the cytoplasmic fraction of Huh-7 cells that were used in our studies. Based on these observations, the results reported here suggest that HAV $3C^{pro}$ reduced the cytoplasmic levels of intact PTB to such a degree that only the activity of the HAV IRES was affected, but not that of the EMCV IRES.

$3C^{pro}$ cleaves PTB

It has been reported that the HAV IRES is associated with La autoantigen, GAPDH, PTB, PABP and PCBP [6,8,12–14]. The latter two proteins were cleaved by HAV $3C^{pro}$ [12,13]. Furthermore, it was shown that PTB is cleaved by polioviral $3C^{pro}$ and that PTB fragments inhibit polioviral IRES-dependent translation [22]. To assess whether the observed suppression of HAV IRES translation might be because of 3C-mediated cleavage of PTB, we tested the levels of endogenous PTB after transient expression of $3C^{pro}$ in Huh-7 cells. As GAPDH was found to suppress HAV IRES translation and to antagonize the enhancing effect of PTB [8], GAPDH levels were tested in parallel. As control for the proteolytic activity of $3C^{pro}$ *in vivo*, cleavage of the poly(A)-binding protein was also analysed. Recombinant $3C^{pro}$ was identified by immunoblot with anti-3C (Fig. 4, left panel) [12,13], and PABP was partially cleaved as demonstrated earlier (Fig. 4, middle panel). Whereas the levels of GAPDH were unchanged (data not shown), a PTB cleavage product of approximately 45 kDa and a slightly faster migrating polypeptide were clearly detectable when HAV $3C^{pro}$ was expressed (Fig. 4, right panel). The extent of host protein cleavage significantly depended on the amount of 3C expressed (compare lanes 1 and 3). Specific PTB cleavage was also observed when the extracts used in Fig. 2 were tested (not shown). Moreover, PTB of Huh-7 cells, the rabbit

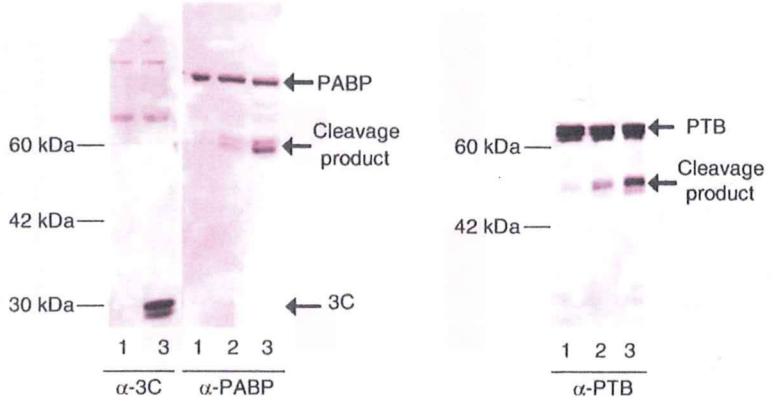

Fig. 4 Hepatitis A virus (HAV) $3C^{pro}$ cleaves the polypyrimidine tract-binding protein (PTB). Huh-7 cells were transfected with pGEM (lanes 1), pGEM-3C (lanes 2) and pEXT7-HAV3C (lanes 3) and infected with vaccinia virus T7. Cell lysates were collected 24 h post-transfection and subjected to immunoblot using anti-3C, anti-poly(A)-binding protein and anti- PTB. As less $3C^{pro}$ was produced by pGEM-3C in comparison with pEXT7-HAV3C, cleavage of host proteins was more pronounced in lanes 3 when compared to lanes2.

reticulocyte lysate, and recombinant PTB produced in *E. coli* was substrate to cleavage-mediated *in vitro* by purified recombinant HAV $3C^{pro}$ (data not shown). Combined with its well-documented translation enhancing effect and binding specificity to stem-loop IIIa of the HAV IRES [6–8], the results strongly suggest that the inhibitory effect of HAV $3C^{pro}$ on HAV IRES translation is because of proteolytic cleavage of PTB.

DISCUSSION

The expression level of the viral proteinase was found to substantially affect the detection of PTB cleavage products (see Fig. 4). Neither in HAV-infected cells nor in cells expressing the HAV replicon were PTB cleavage fragments detectable (not shown). A similar discrepancy was observed for PCBP, another ITAF that is essential for picornaviral translation and the molecular switching to RNA replication [9,23,24]. Whereas PCBP cleavage by recombinant HAV $3C^{pro}$ was clearly shown, PCBP-processing products were not apparent in extracts of HAV-infected cells [9]. Combined, our findings on HAV-3C-mediated cleavage of PCBP and PTB suggest that because of the protracted replication of HAV, very low quantities of $3C^{pro}$ are present in infected cells and cleavage of these host proteins is not discernible. This is in clear contrast to poliovirus whose highly efficient replication resulted in obvious cleavage of both PCBP and PTB [22,24].

The functional domains of PTB are four RNA recognition motifs that all bind short pyrimidine-rich sequences. By binding to different sites on the same RNA molecule, PTB can lead to distinctive RNA restructuring. Such conformational changes are thought to be critical in enabling the ribosomal recruitment in IRES-driven translation initiation. Our constructs do not include the 1–138 nt region of 5′NTR, in which a pyrimidine-rich-tract exists. PTB interacts with stem-loop IIIa of the HAV IRES that contains short polypyrimidine tracts [7]. These binding sites can be bridged by a single PTB molecule, which is an arrangement that favours a role for PTB as an RNA chaperone. It is likely that PTB stabilizes or alters the IRES structure to enable the recruitment of the ribosome and to position it correctly at the start codon.

For poliovirus, direct evidence was provided that PTB cleavage products inhibited IRES-dependent translation [22]. As outlined by the authors, it is possible that PTB fragments may interfere with the binding of intact PTB to poliovirus IRES or that cleaved PTB may no longer function as translational activator that facilitates the recruitment of translational machinery to the IRES element. Although not directly assessed here, it is assumed that suppression of HAV IRES translation is induced by similar mechanism(s). Moreover, in poliovirus-infected Hela cells, PTB cleavage fragments are redistributed to the cytoplasm [22]. As abundant quantities of PTB are present in the cytoplasm of Huh-7 cells used in our study [8], PTB redistribution might not be essential for the effect of PTB cleavage on HAV translation. Yet it is attractive to speculate that the PTB fragment(s) might have altered RNA-binding specificity. For poliovirus IRES translation, an attractive model was put forward for the participation of PTB and PCBP in the molecular switch from viral translation to RNA replication [22]. Supposedly, after viral 3C-mediated cleavage, PTB and PCBP lose their enhancing function. Once IRES translation is stalled, replication of the viral RNA consequently is turned on. Taken together with our earlier observations [9], HAV translation is inhibited indirectly by its own product, $3C^{pro}$, through the proteolytic cleavage of PCBP and PTB.

The HAV 3B and 3C proteins are 23 and 219 amino acids in length, respectively [25]. The 3B moiety was found to be essential for the 3AB interaction with 3CD [26]. It seems that 3BC was more suppressive than 3C in cap-independent translation. Further studies will reveal the 3B function in the interaction with PTB and 3BC. In conclusion, HAV proteinase 3C cleaved PTB and suppressed HAV IRES-dependent translation.

ACKNOWLEDGEMENT

The authors thank Dr S.U. Emerson and Dr J. Miyazaki for pHM175 and pCXN2, respectively.

STATEMENT OF PERSONAL INTERESTS

None of the authors have personal interests relevant to this research to declare.

DECLARATION OF FUNDING INTERESTS

This work was supported by grants 21590829, 21590828 and 21390225 from the Japan Science and Technology Agency, Ministry of Education, Culture, Sports, Science and Technology, Japan (TK, FI and OY) and a grant from Chiba University Young Research-Oriented Faculty Member Development Program in Bioscience Areas (TK).

REFERENCES

1 Martin A, Lemon SM. Hepatitis A virus: from discovery to vaccines. *Hepatology* 2006; 43(2 Suppl. 1): S164–S172.
2 Kanda T, Yokosuka O, Imazeki F *et al.* Amantadine inhibits hepatitis A virus internal ribosomal entry site-mediated translation in human hepatoma cells. *Biochem Biophys Res Commun* 2005; 331(2): 621–629.
3 Schultz DE, Honda M, Whetter LE *et al.* Mutations within the 5′ nontranslated RNA of cell culture adapted hepatitis A virus which enhance cap-independent translation in cultured African green monkey kidney cells. *J Virol* 1996; 70(2): 1041–1049.
4 Semler BL, Waterman ML. IRES-mediated pathways to polysomes: nuclear versus cytoplasmic routes. *Trends Microbiol* 2008; 16(1): 1–5.

5 Cordes S, Kusov Y, Heise T, Gauss-Müller V. La autoantigen suppresses IRES-dependent translation of the hepatitis A virus. *Biochem Biophys Res Commun* 2008; 368(4): 1014–1019.
6 Gosert R, Chang KH, Rijnbrand R *et al.* Transient expression of cellular polypyrimidine-tract binding protein stimulates cap-independent translation directed by both picornaviral and flaviviral internal ribosome entry sites in vivo. *Mol Cell Biol* 2000; 20(5): 1583–1595.
7 Schultz DE, Hardin CC, Lemon SM. Specific interaction of glyceraldehyde 3-phosphate dehydrogenase with the 5′-nontranslated RNA of hepatitis A virus. *J Biol Chem* 1996; 271(24): 14134–14142.
8 Yi M, Schultz DE, Lemon SM. Functional significance of the interaction of hepatitis A virus RNA with GAPDH: opposing effects of GAPDH and polypyrimidine tract binding protein on internal ribosome entry site function. *J Virol* 2000; 74(14): 6459–6468.
9 Zhang B, Seitz S, Kusov Y *et al.* RNA interaction and cleavage of poly(C)-binding protein 2 by hepatitis A virus protease. *Biochem Biophys Res Commun* 2007; 364(4): 725–730.
10 Sawicka K, Bushell M, Spriggs KA, Willis AE. Polypyrimidine-tract-binding protein: a multifunctional RNA-binding protein. *Biochem Soc Trans* 2008; 36(Pt 4): 641–647.
11 Kolupaeva VG, Hellen CU, Shatsky IN. Structural analysis of the interaction of the pyrimidine tract-binding protein with the internal ribosomal entry site of encephalomyocarditis virus and RNAs. *RNA* 1996; 2(12): 1199–1212.
12 Zhang B, Morace G, Gauss-Müller V, Kusov Y. Poly(A) binding protein, C-terminally truncated by the hepatitis A virus proteinase 3C, inhibits viral translation. *Nucleic Acids Res* 2007; 35(17): 5975–5984.
13 Gauss-Müller V, Kusov YY. Replication of a hepatitis A virus replicon detected by genetic recombination in vivo. *J Gen Virol* 2002; 83(Pt 9): 2183–2192.
14 Emerson SU, Lewis M, Govindarajan S *et al.* cDNA clone of hepatitis A virus encoding a virulent virus: induction of viral hepatitis by direct nucleic acid transfection of Marmosets. *J Virol* 1992; 66(11): 6649–6654.
15 Kanda T, Zhang B, Kusov Y *et al.* Suppression of hepatitis A virus genome translation and replication by siRNAs targeting the internal ribosomal entry site. *Biochem Biophys Res Commun* 2005; 330(4): 1217–1223.
16 Kanda T, Yokosuka O, Kato N *et al.* Hepatitis A virus VP3 may activate serum response element associated transcription. *Scand J Gastroenterol* 2003; 38(3): 307–313.
17 Niwa H, Yamamura K, Miyazaki J. Efficient selection for high-expression transfectants with a novel eukaryotic vector. *Gene* 1991; 108(2): 193–200.
18 Kanda T, Steele R, Ray R, Ray RB. Hepatitis C virus core protein augments androgen-receptor mediated signaling. *J Virol* 2008; 88(22): 11066–11072.
19 Chou MY, Underwood JG, Nikolic J *et al.* Multisite RNA binding and release of polypyrimidine tract binding protein during the regulation of c-src neural-specific splicing. *Mol Cell* 2000; 5(6): 949–957.
20 Kaminski A, Jackson RJ. The polypyrimidine tract binding protein (PTB) requirement for internal initiation of translation of cardiovirus RNAs is conditional rather than absolute. *RNA* 1998; 4(6): 626–638.
21 Kim YK, Jang SK. La protein is required for efficient translation driven by encephalomyocarditis virus internal ribosomal entry site. *J Gen Virol* 1999; 80(Pt 12): 3159–3166.
22 Back SH, Kim YK, Kim WJ *et al.* Translation of polioviral mRNA is inhibited by cleavage of polypyrimidine tract-binding proteins executed by polioviral $3C^{pro}$. *J Virol* 2002; 76(5): 2529–2542.
23 Gamarnik AV, Andino R. Switch from translation to RNA replication in a positive-stranded RNA virus. *Genes Dev* 1998; 12(15): 2293–2304.
24 Perera R, Daijogo S, Walter BL *et al.* Cellular protein modification by poliovirus: the two faces of poly(rC)-binding protein. *J Virol* 2007; 81(17): 8919–8932.
25 Totsuka A, Moritsugu Y. Hepatitis A virus proteins. *Intervirology* 1999; 42(2–3): 63–68.
26 Beneduce F, Ciervo A, Kusov Y *et al.* Mapping of protein domains of hepatitis A virus 3AB essential for interaction with 3CD and viral RNA. *Virol* 1999; 264(2): 410–421.

Human Pathology (2009) 40, 1304–1311

ELSEVIER

Human PATHOLOGY

www.elsevier.com/locate/humpath

Original contribution

Distinct expression of polycomb group proteins EZH2 and BMI1 in hepatocellular carcinoma

Yutaka Yonemitsu[a], Fumio Imazeki[a], Tetsuhiro Chiba[b], Kenichi Fukai[a], Yuichiro Nagai[c], Satoru Miyagi[b], Makoto Arai[a], Ryutaro Aoki[a], Masaru Miyazaki[d], Yukio Nakatani[e], Atsushi Iwama[b], Osamu Yokosuka[a,*]

[a]*Department of Medicine and Clinical Oncology, Graduate School of Medicine, Chiba University, Chiba 260-8670, Japan*
[b]*Department of Cellular and Molecular Medicine, Graduate School of Medicine, Chiba University, Chiba 260-8670, Japan*
[c]*Department of Molecular Pathology, Graduate School of Medicine, Chiba University, Chiba 260-8670, Japan*
[d]*Department of General Surgery, Graduate School of Medicine, Chiba University, Chiba 260-8670, Japan*
[e]*Department of Basic Pathology, Graduate School of Medicine, Chiba University, Chiba 260-8670, Japan*

Received 2 August 2008; revised 20 January 2009; accepted 30 January 2009

Keywords:
EZH2;
BMI1;
Hepatocellular carcinoma;
Short hairpin RNA;
MTS assay

Summary Polycomb gene products play a crucial role in the development of highly malignant phenotypes and aggressive cancer progression in a variety of cancers; however, their role in hepatocellular carcinoma remains unclear. First, we analyzed the impact of EZH2 and BMI1 modulation on cell growth of HepG2 cells. 3-(4,5-Dimethylthiazol-2-yl)-5-(3-carboxymethoxyphenyl)-2-(4-sulfophenyl)-2*H*-tetrazolium assays revealed marked growth inhibition after *EZH2* or *BMI1* knockdown. In addition, simultaneous knockdown of these 2 genes further augmented cell growth inhibitory effects. Next, we conducted immnuohistochemical assessment of 86 hepatocellular carcinoma surgical specimens, evaluating the correlation between EZH2 and BMI1 protein expression and clinicopathologic features. High-level EZH2 and BMI1 expression was detected in 57 (66.3%) and 52 tumor tissues (60.5%), respectively. Among these, 48 tumor tissues (55.8%) showed colocalization of EZH2 and BMI1 in almost all tumor cells. The cumulative recurrence rate, but not survival rate, was significantly higher in patients positive for EZH2 ($P = .029$) and BMI1 ($P = .039$) than in their negative counterparts, as determined by Kaplan-Meier analysis. These data indicate that EZH2 and BMI1 may cooperate in initiation and progression of hepatocellular carcinoma.

1. Introduction

Cell-type–specific gene expression profiles are stabilized by changes in chromatin structure and DNA methylation patterns. Polycomb group proteins form multiprotein complexes and serve as a cellular memory system through epigenetic chromatin modifications [1,2]. So far, 2 major polycomb group complexes have been well characterized. Polycomb repressive complex 1 includes BMI1, RNF110/MEL18, HPH, CBX2/HPC1, Ring1A, and Rind1B, and polycomb repressive complex 2 includes EED, EZH2, and SUZ12. The polycomb repressive complex 1 and polycomb repressive complex 2 possess H2A-K119 ubiquitin E3 ligase activity and H3-K27 methyltransferase activity, respectively. BMI1, which is part of the polycomb repressive complex 1, contributes to the enhancement of RING1-mediated H2A-K119 ubiquitin E3 ligase activity. EZH2, a key molecule of

* Corresponding author.
E-mail address: yokosukao@faculty.chiba-u.jp (O. Yokosuka).

0046-8177/$ – see front matter © 2009 Elsevier Inc. All rights reserved.
doi:10.1016/j.humpath.2009.01.017

polycomb repressive complex 2, possesses histone methyltransferase activity and causes methylation at lysine residues of histone H3 (H3-K27). Both histone modifications contribute to polycomb group gene silencing. Although no physical associations have been demonstrated between the 2 complexes, H3-K27 methylation serves as a binding site for the recruitment of the polycomb repressive complex 1. Thus, the 2 polycomb group complexes could function in a cooperative manner to maintain gene silencing [1,2].

Polycomb repressive complex 1 has been implicated in stem cell self-renewal [1,2], a process by which epigenetic cellular memory is precisely inherited by daughter cells through cell division. Among polycomb repressive complex 1 components, we have demonstrated that BMI1 plays a central role in the inheritance of self-renewal of hematopoietic stem cells in both loss-of-function and gain-of-function analyses [3]. It is well recognized that polycomb repressive complex 1 transcriptionally represses tumor suppressor genes such as the Ink4b-Arf-Ink4a locus, which functions as a barrier to eliminate oncogenic cells by triggering apoptosis or cellular senescence [1,4]. We have demonstrated that tight repression of Ink4a-Arf in hematopoietic stem cells is essential to maintain the self-renewing capacity of hematopoietic stem cells [5]. On the other hand, there is increasing evidence that up-regulation of polycomb group proteins is deeply involved in tumor development. EZH2 is reportedly involved in the pathogenesis of malignant lymphoma and multiple myeloma [6,7]. BMI1 was initially identified as a c-myc–cooperating protooncogene in murine lymphomas [8], and increased levels of BMI1 expression has been implicated not only in human lymphoma but also in several types of leukemia [9-11]. Moreover, coexpression of EZH2 and BMI1 appears to be associated with the degree of malignancy in B-cell non–Hodgkin lymphoma [12]. Of importance, recent studies demonstrated that the increased expression of EZH2 proteins correlates with progression and poor prognosis of solid tumors such as prostate cancer and breast cancer [13-15].

In the present study, we first examined the cell growth activity of hepatocellular carcinoma cells stably expressing short hairpin RNAs against EZH2 and BMI1 in culture. Next, we conducted immunohistochemical analyses to estimate the expression levels of polycomb group proteins EZH2 and BMI1 in hepatocellular carcinoma. The cumulative survival rates and recurrent rates were analyzed using the Kaplan-Meier method to ask whether these molecules could be novel biologic markers.

2. Materials and methods

2.1. Cell culture

The hepatocellular carcinoma cell line HepG2 was cultured in Dulbecco's modified Eagle's medium (Invitrogen Life Technologies, Carlsbad, CA) supplemented with 10% fetal bovine serum and 1% penicillin/streptomycin (Invitrogen).

2.2. Lentiviral production and transduction

Lentiviral vectors (CS-H1-short hairpin RNA EF-1α-EGFP and CS-CDF-RfA-ERP) expressing short hairpin RNA that targets human EZH2 (target sequence: 5′-GGAAAGAACGGAAATCTTA-3′), human BMI1 (target sequence: 5′-GAGAAGGAATGGTCCACTT-3′), and luciferase were constructed. Recombinant lentiviruses were produced as described elsewhere [3]. The cells were transduced with viruses in the presence of protamine sulfate.

2.3. Immunocytochemical analyses

HepG2 cells were fixed with methanol. After blocking in 10% goat serum, the cells were stained with a primary rabbit anti-EZH2 antibody (Zymed, San Francisco, CA) and a primary mouse anti-BMI1 antibody (Upstate Biotechnology, Lake Placid, NY) for 12 hours at 4°C. The cells then were washed and incubated with Alexa-555–conjugated goat anti-rabbit immunoglobulin G (IgG) (Molecular Probes, Eugene, OR) or Alexa-488–conjugated goat anti-mouse IgG (Molecular Probes), as appropriate, for 2 hours at room temperature. After being washed in phosphate-buffered saline (PBS), the cells were coverslipped with a mounting medium containing 4′,6-diamidino-2-phenylindole (DAPI) dihydrochloride (Vector Laboratories, Burlingame, CA).

2.4. Measurement of cell proliferation by 3-(4,5-dimethylthiazol-2-yl)-5-(3-carboxymethoxyphenyl)-2-(4-sulfophenyl)-2H-tetrazolium assay

Cell growth of HepG2 cells after stable knockdown of EZH2 and/or BMI1 was measured by 3-(4,5-dimethylthiazol-2-yl)-5-(3-carboxymethoxyphenyl)-2-(4-sulfophenyl)-2H-tetrazolium (MTS) assay. For this, we seeded cells in a 6-well plate at a density of 1×10^4 cells per well. MTS assays were performed in triplicate using the Cell Titer 96 Aqueous One Solution Cell Proliferation kit (Promega, Madison, WI) at culture days 2, 3, 4, and 5.

2.5. Patients and surgical specimens

Eighty-six patients who underwent surgical resection for hepatocellular carcinoma at Chiba University, Chiba, Japan, hospital were analyzed in this study. Informed consent for research use of the specimens was obtained for all cases. There were 73 male patients and 13 female patients with an average age of 63 ± 11 years (52-80 years). Among these, 32 cases had liver cirrhosis and 50 cases showed chronic hepatitis with mild to moderate activities. Liver damage of the patients was due to autoimmune disorder (n = 1), hepatitis B virus (HBV) (n = 19), hepatitis C virus (HCV)

(n = 38), both HBV and HCV (n = 2), and unknown etiology (n = 26). Paraffin-embedded sections of the tumors and surrounding nontumor liver tissues were examined by hematoxylin-eosin (H&E) staining and immunohistochemistry.

2.6. Immunohistochemical analyses

After deparaffinization and inhibition of endogenous peroxidase activities, the pathologic specimens of surgically resected tumors were stained with rabbit anti-EZH2 (1:100, Zymed), mouse anti-BMI1 (1:100, Upstate Biotechnology) or mouse anti–Ki-67 (1:50; Santa Cruz Biotechnology, Santa Cruz, CA) antibodies. Before incubation with the primary antibodies, antigen retrieval was performed with ethylenediaminetetraacetic acid buffer (pH 8.0) in a pressure cooker at 100°C for 1 minute. The proteins were detected using ImmPRESS peroxidase micropolymer staining kits (Vector Laboratories) and 3,3′-diaminobenzidine substrate according to the manufacturer's instructions. To investigate the colocalization of EZH2 and BMI1, we simultaneously stained the clinical specimens with indicated antibodies. Subsequently, they were stained with Alexa-555–conjugated goat anti-rabbit IgG (Molecular Probes) and Alexa-488–conjugated goat anti-mouse IgG (Molecular Probes), respectively.

2.7. Statistical analyses

Statistical differences between 2 groups in MTS assays were analyzed using the Student t test. The correlations between the expression of polycomb group proteins and clinicopathologic features were assessed using the χ^2 test and Student t test to analyze qualitative and quantitative data, respectively. The cumulative survival and recurrent rates were analyzed by the Kaplan-Meier method, and the statistical significance between the 2 groups positive and

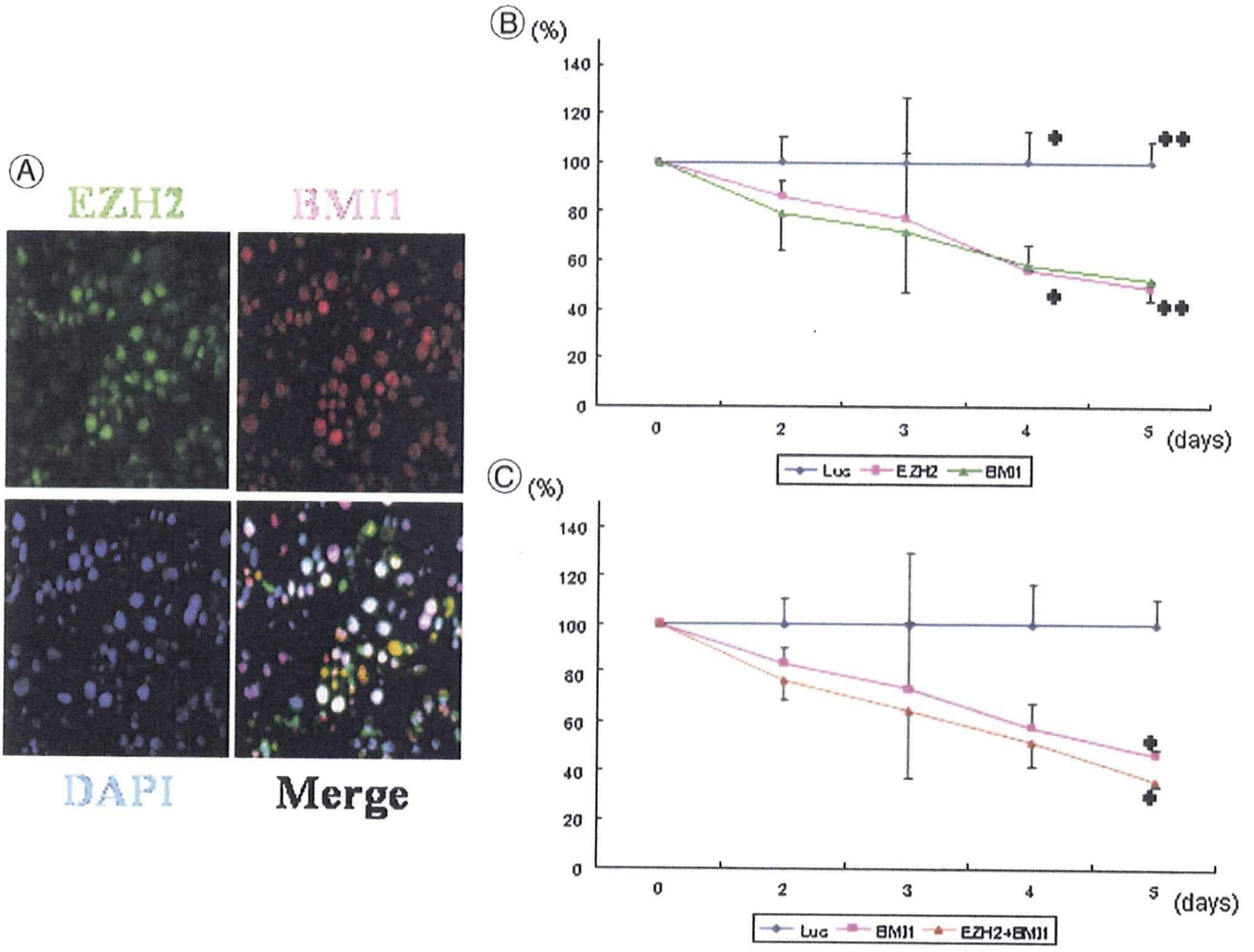

Fig. 1 Loss-of-function assays of EZH2 and BMI1 in HepG2 cells. (A) Immunocytochemical analyses of EZH2 and BMI1. Immunofluorescent labeling of EZH2 (green), BMI1 (red), and nuclear DAPI staining (blue) is merged. (B) Cell growth inhibition of EZH2 or BMI1 knockdown HepG2 cells compared with luciferase knockdown HepG2 cells as a control. Mean ± SD values are shown for each group, $*P < .05$, $**P < .005$. (C) Augmented growth inhibition of both EZH2 and BMI1 knockdown HepG2 cells. Mean ± SD values are shown for each group, $*P < .005$.

negative for polycomb group immunostaining was analyzed using the Wilcoxon test. Cox proportional regression analysis was performed to estimate rate ratios for the effect of EZH2 and BMI1 staining in tumors for recurrence. Potential risk factors assessed for recurrence included the following variables: BMI1 in tumors (presence versus absence), EZH2 in tumors (presence versus absence), sex (male versus female), age (>65 versus ≤65 years), size of tumors (>45 versus ≤45 mm), differentiation (poorly versus well, moderately), TNM stage [16] (I + II versus III + IVa), protein induced by vitamin K absence II (PIVKA II) level (>100 versus ≤100 mAU/mL), α-fetoprotein (AFP) level (>40 versus ≤40 mg/mL), etiology (HBV and HCV versus HBV alone, HCV alone, non-HBV, and non-HCV), chronic hepatitis (versus liver cirrhosis), aspartate aminotransferase (AST) level (>50 versus ≤50 IU/L), alanine aminotransferase (ALT) level (>50 versus ≤50 IU/L), total bilirubin level (>1.0 versus ≤1.0 mg/dL), albumin level (>3.8 versus ≤3.8 g/dL), platelet count (>15 × 10^9/L versus ≤15 × 10^9/L), prothrombin time (>80% versus ≤80%), the presence of portal invasion (versus no portal invasion), and tumor number (>2 versus ≤2). Variables statistically significant by univariate Cox proportional regression analysis were further studied by multivariate analysis. The differences were considered significant at $P < .05$.

3. Results

3.1. Stable short hairpin RNA-mediated knockdown of EZH2 and BMI1 mediated growth inhibition in HepG2 cells

To examine the basal expression of EZH2 and BMI1 in hepatocellular carcinoma cells, we conducted dual immunocytochemical analyses in HepG2 cells. EZH2 and BMI1 were widely detected in the nucleus and were coexpressed in more than 70% of HepG2 cells (Fig. 1A). To gain insight into the role of the polycomb gene products in HepG2 cells, we performed loss-of-function assays using lentivirus-mediated knockdown techniques. MTS assays showed that cell growth activity was consistently repressed, after EZH2 and BMI1 knockdown, for the 5 days of the observation period (Fig. 1B). Cell growth activity at days 2, 3, 4, and 5 was 86% ± 6.2%, 77% ± 27%, 56% ± 10%, and 49% ± 2.4%, respectively, after EZH2 knockdown and 79% ± 15%, 72% ± 25%, 58% ± 2.5%, and 52% ± 8.3%, respectively, after BMI1 knockdown compared with the luciferase knockdown cells, with there being a statistically significant difference at day 4 ($P < .05$) and 5 ($P < .005$) in the case of EZH2 or BMI1 knockdown. Intriguingly, simultaneous knockdown of EZH2 and BMI1 mediated an even greater degree of growth inhibition of HepG2 cells (Fig. 1C). Cell growth activity at days 2, 3, 4, and 5 was 77% ± 7.9%, 65% ± 27%, 52% ± 10%, and 36% ± 1.8%, respectively, after simultaneous knockdown compared with luciferase knockdown cells, with there being a statistically significant difference at day 5 ($P < .005$) between knockdown of both EZH2 and BMI1 and that of BMI1 alone.

Table 1 EZH2 and BMI1 expression in hepatocellular carcinoma and equivalent nontumor tissues

	Tumor	Nontumor
EZH2	57/86 (66.3%)*	5/86 (5.8%)*
BMI1	52/86 (60.5%)**	4/86 (4.7%)**

*, **$P < .05$.

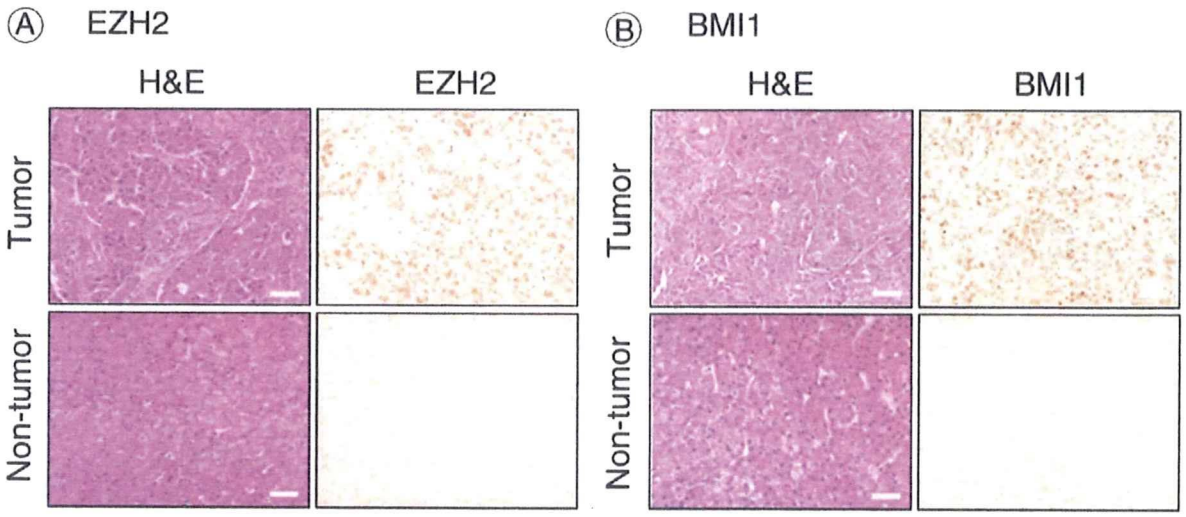

Fig. 2 Representative histopathologic analyses of EZH2 and BMI1. (A) H&E staining and immunohistochemical analysis of EZH2 in hepatocellular carcinoma tissue and the corresponding nontumor tissue. (B) H&E staining and immunohistochemical analysis of BMI1 in hepatocellular carcinoma tissue and the corresponding nontumor tissue (scale bar = 50 μm).

Table 2 The expression pattern of EZH2 and BMI1 in tumor and nontumor tissues

	Tumor				Nontumor			
	BMI1+	BMI1−	Total	*P*	BMI1+	BMI1−	Total	*P*
EZH2+	48	9	57	<.01	0	5	5	>.99
EZH2−	3	26	29		4	77	81	
Total	51	35	86		4	82	86	

3.2. Preferential expression of EZH2 and BMI1 in hepatocellular carcinoma samples

We evaluated the expression levels of polycomb group proteins EZH2 and BMI1 in hepatocellular carcinoma tissues and the corresponding nontumor tissues obtained from 86 patients by histopathologic analyses. Representative immunohistochemical staining of EZH2 and BMI1 is shown in Fig. 2A and B. The expression of EZH2 and BMI1 was diffusely detected in the nuclei of cancer cells, and no patients showed focal expression of these proteins in tumor tissues.

Fifty-seven (66.3%) of 86 hepatocellular carcinoma samples were positive for EZH2, whereas only 5 (5.8%) of 86 nontumor samples showed EZH2 expression ($P < .01$) (Table 1). On the other hand, BMI1 expression was detected in 52 (60.5%) of 86 hepatocellular carcinoma samples, whereas its expression was detected in only 4 (4.7%) of 86 nontumor samples ($P < .01$) (Table 1). Of importance, 48 (55.8%) of 86 hepatocellular carcinoma samples expressed both EZH2 and BMI1 (Table 2). Consequently, 26 (30.2%) of 86 samples did not express either protein. These results showed a statistically significant difference with respect to EZH2-positive ratio between BMI1-positive and BMI1-negative tumor tissues ($P < .01$). In contrast, 77 (89.5%) of 86 nontumor samples were negative for both EZH2 and BMI1 (Table 2). These results indicate that the expression of EZH2 and BMI1 is preferentially up-regulated in hepatocellular carcinoma samples, and their expression patterns could segregate hepatocellular carcinoma samples into subgroups.

3.3. Coexpression of EZH2 and BMI1 in hepatocellular carcinoma tissues

To determine whether EZH2 and BMI1 are coexpressed in the same hepatocellular carcinoma cells, we performed dual immunofluorescence staining on 10 randomly selected hepatocellular carcinoma tissues that were positive for both EZH2 and BMI1 by conventional immunohistochemical analysis. As shown in Fig. 3, EZH2 and BMI1 were detected in the nucleus and were coexpressed in more than 70% of hepatocellular carcinoma cells in all samples analyzed. These results strongly indicate cooperative contributions of EZH2 and BMI1 to the development and progression of hepatocellular carcinoma.

3.4. Correlation between the expression of EZH2 or BMI1 and that of Ki-67

We performed immunohistochemical analysis of Ki-67 in tumor and nontumor tissues and compared the results with those of EZH2 and BMI1 (Table 3). EZH2 was positive in 47 (80%) of 59 Ki-67–positive tumors and in 10 (37%) of 27 Ki-67–negative tumors ($P = .0002$). BMI1 was also positive in 44 (75%) of 59 Ki-67–positive tumors and in 8 (30%) of 27 Ki-67–negative tumors ($P = .0001$). In nontumor tissues, the staining of Ki-67 was found only in 11 cases, and we found no correlation between these 2 proteins and Ki-67 (Table 3).

3.5. Relationship between EZH2 or BMI1 expression and clinicopathologic features

We next evaluated the relationship between increased expression of polycomb group proteins and clinicopathologic parameters of the 86 hepatocellular carcinoma patients (Table 4). Significant correlation was observed between increased EZH2 expression in hepatocellular carcinoma tissues and hypoalbuminemia ($P = .01$) or advanced TNM stage ($P = .04$). In contrast, increased BMI1 expression in the

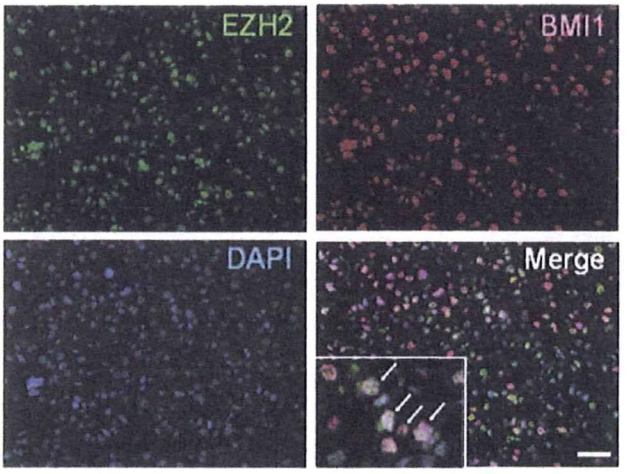

Fig. 3 Representative dual immunostaining of EZH2 (green) and BMI1 (red) in hepatocellular carcinoma tissue and the corresponding nontumor tissue. The nuclei were stained with DAPI (blue). Arrows indicate a typical nucleus positive for EZH2, BMI1, and DAPI (scale bar = 50 μm).

Table 3 Correlation between the expression of EZH2 or BMI1 and that of Ki-67

	Tumor				Nontumor			
	Ki-67+	Ki-67−	Total	*P*	Ki-67+	Ki-67−	Total	*P*
EZH2+	47	10	57	.0002	1	4	5	>.50
EZH2−	12	17	29		10	71	81	
Total	59	27	86		11	75	86	
BMI1+	44	8	52	.0001	1	3	4	.43
BMI1−	15	19	34		10	72	82	
Total	59	27	86		11	75	86	

hepatocellular carcinoma samples had no significant correlation with clinicopathologic factors.

3.6. Prognostic value of EZH2 or BMI1 expression in hepatocellular carcinoma patients

To elucidate the role of polycomb group proteins in hepatocellular carcinoma progression, we performed prognostic analyses of 61 hepatocellular carcinoma patients in whom curative operation was conducted and whose postoperative course could be followed. The cumulative recurrent rates and survival rates were analyzed by the Kaplan-Meier method (Fig. 4A-D). During the follow-up period (27.2 ± 19.6 months), 39 patients developed a recurrence of hepatocellular carcinoma and 19 patients died from relapsed hepatocellular carcinoma. Our results demonstrated higher cumulative recurrence rates in EZH2-positive patients than in EZH2-negative patients (P = .029). In contrast, the cumulative survival rates showed no significant differences between EZH2-positive and EZH2-negative patients. Of interest, results of the prognostic analysis correlating BMI1 expression were similar to those of the EZH2 expression-based analysis. The cumulative recurrence rates were higher in BMI1-positive patients than in BMI1-negative patients (P = .039), although the difference in survival rates between the 2 groups was not significant. Given that EZH2 and BMI1 are frequently coexpressed in the same samples, these prognostic findings appear quite reasonable.

Table 4 Correlation between polycomb group protein expression and clinicopathologic background in 86 hepatocellular carcinoma samples

Variables	EZH2 expression			BMI1 expression		
	Negative (n = 29)	Positive (n = 57)	*P*	Negative (n = 34)	Positive (n = 52)	*P*
Sex (male/female)	27/2	46/11	.13	31/3	42/10	.46
Age (y)	64.7 ± 9.8	62.6 ± 12.5	.45	63.6 ± 11.6	63.1 ± 11.8	.86
Liver function						
AST (IU/L)	66.8 ± 79.4	94.8 ± 126.0	.30	67.4 ± 75.0	97.2 ± 131.2	.25
ALT (IU/L)	71.4 ± 64.8	90.4 ± 122.3	.46	71.9 ± 64.3	92.0 ± 126.8	.42
Total bilirubin (mg/dL)	1.00 ± 0.38	1.12 ± 0.64	.39	0.96 ± 0.36	1.15 ± 0.66	.15
Albumin (g/dL)	4.02 ± 0.48	3.70 ± 0.53	.01[a]	3.92 ± 0.50	3.74 ± 0.55	.14
Prothrombin time (%)	84.4 ± 12.9	84.7 ± 19.3	.95	83.6 ± 12.5	85.1 ± 20.0	.76
Platelet (×10^4/mL)	15.60 ± 6.62	15.89 ± 6.66	.85	15.94 ± 6.88	15.70 ± 6.5	.88
PIVKA II (mAU/mL)	4027.0 ± 9934.8	5040.6 ± 12 873.8	.76	5654.6 ± 13 844.7	4250.1 ± 11 063.9	.65
AFP (mg/mL)	108.0 ± 181.6	9570.6 ± 37 690.7	.21	3710.9 ± 19 937.8	8283.1 ± 36 691.8	.53
Tumor factors						
Tumor size (mm)	47.4 ± 33.5	51.4 ± 33.6	.63	51.3 ± 34.5	49.4 ± 33.0	.81
No.	1.19 ± 0.51	1.40 ± 0.61	.18	1.26 ± 0.59	1.38 ± 0.58	.40
VP (+) (%)	3/19 (15.8%)	17/50 (34%)	.23	7/24 (29.2%)	13/45 (28.9%)	>.99
Well/moderate/poorly[b]	4/16/4	6/36/9	.84	5/20/4	5/32/9	.64
TNM (I/II/III/IVa)	5/15/4/0	5/25/20/8	.04[a]	4/17/8/0	6/23/16/8	.14
Etiology						
AIH/B/C/B and C/BC (−)	0/5/12/0/12	1/14/26/2/14	.63	1/6/14/0/13	0/13/24/2/13	.42
CH/LC	16/11	34/21	.81	21/11	29/21	.64

Abbreviations: VP, invasion to portal vein; AIH, autoimmune hepatitis; CH, chronic hepatitis; LC, liver cirrhosis; B, hepatitis B; C, hepatitis C.
NOTES: Reference range—AST, 10 to 35 IU/L; ALT, 5 to 40 IU/L; total bilirubin, 0.4 to 1.2 mg/dL; albumin, 3.9 to 5.2 g/dL; prothrombin time, 70% to 140%; platelet, 15 to 35 × 10^4/mL; PIVKA II, <40 mAU/mL; AFP, <20 ng/mL.

[a] Statistically significant.

[b] Histologic differentiation of the tumor.

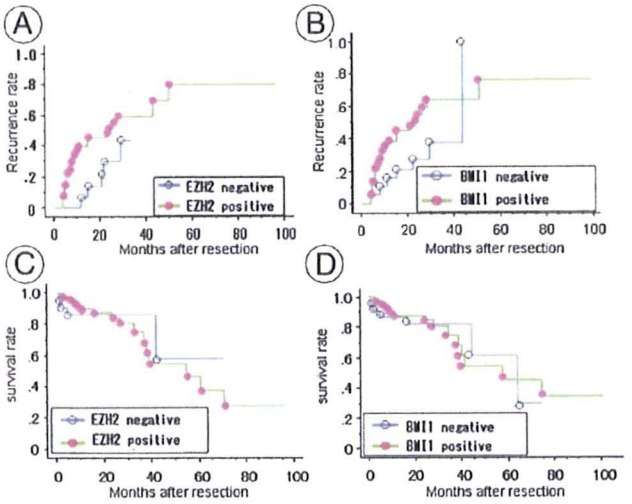

Fig. 4 Kaplan-Meier curves for the prognostic analyses. A and B, Cumulative recurrence rate with regard to EZH2 expression (A) and BMI1 expression (B). C and D, Cumulative survival rate with regard to EZH2 expression (C) and BMI1 expression (D).

The potential risk factors affecting tumor recurrence were analyzed by univariate Cox proportional hazards regression, and variables of P value less than 0.1 (the presence of BMI1, risk ratio, 2.3, $P = .053$; the presence of EZH2, risk ratio, 2.5, $P = .060$; age ≤65 years, risk ratio, 2.4, $P = .018$; AFP >40 mg/mL, risk ratio, 2.5, $P = .013$; albumin ≤3.8 mg/dL, risk ratio, 2.3, $P = .020$; the presence of portal vein invasion, risk ratio, 2.1, $P = .050$; TNM stage I + II, risk ratio, 0.40, $P = .015$) were further studied by multivariate analysis. However, we found that no variables examined in this multivariate analysis showed a statistically significant correlation with recurrence (the presence of BMI1, risk ratio, 1.4, $P = .51$; the presence of EZH2, risk ratio, 1.6, $P = .47$; age ≤65 years, risk ratio, 2.4, risk ratio, 2.0, $P = .07$; AFP >40 mg/mL, risk ratio, 2.0, $P = .12$; albumin ≤3.8 mg/dL, risk ratio, 2.2, $P = .11$; the presence of portal vein invasion, risk ratio, 0.64, $P = .43$; TNM stage I + II, risk ratio, 0.52, $P = .10$).

We found no effect on survival and recurrence in tumors that simultaneously expressed both EZH2 and BMI1 as compared with those that expressed only one of these proteins ($P = .61$ for recurrence and $P = .58$ for survival, as determined by Kaplan-Meier analysis).

4. Discussion

Hepatocellular carcinoma is one of the most common malignancies, and chronic viral infection by hepatitis B or C virus is well recognized as a major risk factor [17]. Therapeutic advancements such as nucleotide analogues and interferon has successfully improved hepatitis viremia and reduced the incidence of hepatocellular carcinoma, but the mortality rate of hepatocellular carcinoma remains high in spite of recent advances in cancer therapy [18]. In hepatocarcinogenesis, it appears that repeated injury and regeneration of damaged liver cells induce genetic and epigenetic dysregulation, which ultimately contribute to cancer development [19,20]. Recent studies highlight the pivotal role of polycomb group proteins in cancer [1]. However, our knowledge on their implications in hepatocarcinogenesis remains limited [21].

At first, we examined the growth activity of HepG2 cells in loss-of-function assays. The MTS assays showed that EZH2 or BMI1 knockdown mediated significant cell growth inhibition. This finding appears to be consistent with previous observations suggesting a role for EZH2 or BMI1 in a variety of immortalized and transformed cells [6,7,22]. Interestingly, knockdown of both EZH2 and BMI1 augmented cell growth inhibition, which indicated that the function of EZH2 might partly differ from that of BMI1 in molecular mechanisms underlying proliferation of hepatocellular carcinoma cells.

On the other hand, immunohistochemical analyses showed that increased expression of either EZH2 or BMI1 protein was observed in 60 (69.8%) of 86 hepatocellular carcinoma samples. Meanwhile, only 5.8% and 4.7% of surrounding nontumor tissues expressed EZH2 and BMI1, respectively. These results unveil preferential up-regulation of polycomb group protein expression during hepatocarcinogenesis and might implicate a special role for polycomb group proteins in the development and progression of hepatocellular carcinoma. Given that EZH2 and BMI1 were frequently coexpressed in the same samples, there might be functional crosstalk between EZH2 and BMI1 in the pathogenesis of hepatocellular carcinoma. Conversely, 26 (30.2%) of 86 samples exhibited expression of neither protein, which might be reflective of inherent heterogeneity with respect to origin of hepatocellular carcinoma and/or underlying molecular mechanisms.

Analyses of EZH2 mRNA expression in hepatocellular carcinoma samples based on real-time reverse transcriptase polymerase chain reaction have previously documented no significant correlation between EZH2 expression and disease-free survival [21]. Recently, another group reported that overexpression of EZH2 and BMI1 is associated with aggressive biologic behavior including vascular invasion and lymph node metastasis [23,24]. To examine whether protein expression of EZH2 and BMI1 are good biomarkers for recurrence and survival in our samples, we conducted prognostic analyses. The present analyses demonstrate that increased expression of both EZH2 and BMI1 proteins significantly correlated with recurrence after hepatectomy ($P = .029$ and $P = .039$, respectively), although there was no significant correlation between the expression of these polycomb group proteins and survival. Analyses of clinicopathologic parameters showed lower levels of serum albumin and advanced stage of TNM in EZH2-positive patients compared with EZH2-negative patients, which might indicate advanced liver dysfunction and tumor stage in EZH2-positive patients. In contrast, the significant

correlation between high EZH2 expression and portal vein invasion of the tumor, which was previously reported by mRNA expression-based analyses [21], was not detected in this study ($P = .23$).

In conclusion, our studies showed that polycomb proteins, in particular, EZH2 and BMI1, can have a strong effect on proliferation of hepatocellular carcinoma cells and that simultaneous knockdown of EZH2 and BMI1 has more marked effect on cell growth inhibition than knockdown of either protein alone. Immunohistochemical analyses further demonstrated a clear association between EZH2 and BMI1 expression and the development and progression of hepatocellular carcinoma, as well as recurrence after curative surgery. Thus, EZH2 and BMI1 could be target molecules in the development of new treatment strategies against hepatocellular carcinoma.

Acknowledgments

The authors thank Dr Huroyuki Miyoshi (RIKEN, Tsukuba, Japan) for providing lentiviral vectors and Dr Yoh Zen (Kanazawa University, Kanazawa, Japan) for technical assistance in immunohistochemical analyses.

References

[1] Valk-Lingbeek ME, Bruggeman SWM, van Lohuizen M. Stem cells and cancer: the polycomb connection. Cell 2004;118:409-18.

[2] Sparmann A, van Lohuizen M. Polycomb silencers control cell fate, development and cancer. Nat Rev Cancer 2006;6:846-56.

[3] Iwama A, Oguro H, Negishi M, et al. Enhanced self-renewal of hematopoietic stem cells mediated by the polycomb gene product, Bmi-1. Immunity 2004;21:843-51.

[4] Gil J, Peters G. Regulation of the INK4b-ARF-INK4a tumour suppressor locus: all for one or one for all. Nat Rev Mol Cell Biol 2006;7:667-77.

[5] Oguro H, Iwama A, Morita Y, Kamijo T, van Lohuizen M, Nakauchi H. Differential impact of Ink4a and Arf on hematopoietic stem cells and their bone marrow microenvironment in Bmi1-deficient mice. J Exp Med 2006;203:2247-53.

[6] Visser HP, Gunster MJ, Kluin-Nelemans HC, et al. The Polycomb group protein EZH2 is upregulated in proliferating, cultured human mantle cell lymphoma. Br J Haematol 2001;112:950-8.

[7] Croonquist PA, Van Ness B. The polycomb group protein enhancer of zeste homolog 2 (*EZH2*) is an oncogene that influences myeloma cell growth and the mutant ras phenotype. Oncogene 2005;24:6269-80.

[8] van Lohuizen M, Verbeek S, Scheijen B, Wientjens E, van der Gulden H, Berns A. Identification of cooperating oncogenes in Eμ-myc transgenic mice by provirus tagging. Cell 1991;65:737-52.

[9] Smith KS, Chanda SK, Lingbeek M, et al. Bmi-1 regulation of INK4A-ARF is a downstream requirement for transformation of hematopoietic progenitors by E2a-Pbx1. Mol Cell 2003;12:393-400.

[10] Mohty M, Yong AS, Szydlo RM, Apperley JF, Melo JV. The polycomb group BMI1 gene is a molecular marker for predicting prognosis of chronic myeloid leukemia. Blood 2007;110:380-3.

[11] Chowdhury M, Mihara K, Yasunaga S, Ohtaki M, Takihara Y, Kimura A. Expression of Polycomb-group (PcG) protein BMI-1 predicts prognosis in patients with acute myeloid leukemia. Leukemia 2007;21:1116-22.

[12] van Kemenade FJ, Raaphorst FM, Blokzijl T, et al. Coexpression of BMI-1 and EZH2 polycomb-group proteins is associated with cycling cells and degree of malignancy in B-cell non–Hodgkin lymphoma. Blood 2001;97:3896-901.

[13] Varambally S, Dhanasekaran SM, Zhou M, et al. The polycomb group protein EZH2 is involved in progression of prostate cancer. Nature 2002;419:624-9.

[14] Kleer CG, Cao Q, Varambally S, et al. EZH2 is a marker of aggressive breast cancer and promotes neoplastic transformation of breast epithelial cells. Proc Natl Acad Sci U S A 2003;100:11606-11.

[15] Kim JH, Yoon SY, Jeong SH, et al. Overexpression of Bmi-1 oncoprotein correlates with axillary lymph node metastases in invasive ductal breast cancer. Breast 2004;13:383-8.

[16] Liver Cancer Study Group of Japan. The general rules for the clinical and pathological study of primary liver cancer. 2nd English ed. Tokyo: Kanehara & Co., Ltd.; 2003.

[17] Wang BE, Ma WM, Sulaiman A, et al. Demographic, clinical, and virological characteristics of hepatocellular carcinoma in Asia: survey of 414 patients from four countries. J Med Virol 2002;67:394-400.

[18] Colombo M, Donato MF. Prevention of hepatocellular carcinoma. Semin Liver Dis 2005;25:155-61.

[19] Bruix J, Boix L, Sala M, Llovet JM. Focus on hepatocellular carcinoma. Cancer Cell 2004;5:215-9.

[20] Roberts LR, Gores GJ. Hepatocellular carcinoma: molecular pathways and new therapeutic targets. Semin Liver Dis 2005;25:212-25.

[21] Sudo T, Utsunomiya T, Mimori K, et al. Clinicopathological significance of EZH2 mRNA expression in patients with hepatocellular carcinoma. Br J Cancer 2005;92:1754-8.

[22] Chen Y, Lin MC, Yao H, et al. Lentivirus-mediated RNA interference targeting enhancer of zeste homolog 2 inhibits hepatocellular carcinoma growth through down-regulation of stathmin. Hepatology 2007;46:200-8.

[23] Sasaki M, Ikeda H, Itatsu K, et al. The overexpression of polycomb group proteins Bmi1 and EZH2 is associated with the progression and aggressive biological behavior of hepatocellular carcinoma. Lab Invest 2008;00 00:1-10.

[24] Sasaki M, Yamaguchi J, Itatsu K, Ikeda H Nakanuma Y. Over-expression of polycomb group protein EZH2 relates to decreased expression of $P16^{INK4a}$ in cholangiocarcinogenesis in hepatolithiasis. J Pathol 2008;215:175-83.

Liver International ISSN 1478-3223

CLINICAL STUDIES

Phylogenetic analysis of hepatitis A virus in sera from patients with hepatitis A of various severities

Keiichi Fujiwara[1], Hiroshige Kojima[1], Yutaka Yonemitsu[1], Shin Yasui[1], Fumio Imazeki[1], Makoto Miki[2], Kazuyuki Suzuki[3], Isao Sakaida[4], Kiwamu Okita[4], Eiji Tanaka[5], Masao Omata[6] and Osamu Yokosuka[1]

1 Department of Medicine and Clinical Oncology, Graduate School of Medicine, Chiba University, Chiba, Japan
2 Department of Internal Medicine, Yokohama Higashi National Hospital, Kanagawa, Japan
3 First Department of Internal Medicine, Iwate Medical University, Iwate, Japan
4 Department of Gastroenterology and Hepatology, Yamaguchi University School of Medicine, Yamaguchi, Japan
5 Department of Medicine, Shinshu University School of Medicine, Nagano, Japan
6 Department of Gastroenterology, Faculty of Medicine, University of Tokyo, Tokyo, Japan

Keywords
2B – 2C – 5′NTR – fulminant hepatitis – hepatitis A – hepatitis A virus

Abbreviations
AH, acute hepatitis; AHs, acute hepatitis severe type; FH, fulminant hepatitis; HAV, hepatitis A virus; PT, prothrombin time.

Correspondence
Keiichi Fujiwara, MD, PhD, Department of Medicine and Clinical Oncology, Graduate School of Medicine, Chiba University, 1-8-1 Inohana, Chuo-ku, Chiba 260-8670, Japan
Tel: +81 43 226 2083
Fax: +81 43 226 2088
e-mail: fujiwara-cib@umin.ac.jp

Received 13 August 2008
Accepted 4 October 2008

DOI:10.1111/j.1478-3231.2008.01919.x

Abstract

Background: We analysed the association of the 5′ nontranslated region (5′NTR), nonstructural proteins 2B and 2C of the hepatitis A virus (HAV) genome, whose mutations have previously been shown to be important for enhanced replication in cell culture systems, in order to align all our data and examine whether genomic differences in HAV are responsible for the range of clinical severities. *Methods:* Our accumulated HAV strains of 5′NTR [nucleotide(nt) 200 and 500], entire 2B and 2C from 25 Japanese patients with sporadic hepatitis A, consisting of seven patients with fulminant hepatitis (FH), five with severe acute hepatitis (AHs) and 13 with self-limited acute hepatitis (AH), in whom the sequences of all three regions were available, were subjected to phylogenetic analysis. *Results:* Fulminant hepatitis patients had fewer nucleotide substitutions in 5′NTR, had a tendency to have more amino acid (aa) substitutions in 2B and had fewer aa substitutions in 2C than AH patients. Four FH and two AHs with a higher viral replication were located in the near parts of the phylogenetic trees, indicating the association between the severity of hepatitis A and genomic variations in 5′NTR, 2B and 2C of HAV. *Conclusions:* Our study suggests that genetic variations in HAV not in one specific region but in 5′NTR, 2B and 2C might cooperatively influence replication of the virus, and thereby affect virulence. Viral factors should be considered and examined when discussing the mechanisms responsible for the severity of hepatitis A.

Hepatitis A is still a major problem worldwide, not only in underdeveloped countries but also in industrialized nations. Because of improvements in sanitation, there have been no hepatitis A epidemics in Japan in recent years. However, sporadic cases of hepatitis A have not been rare of late. Although the majority of hepatitis A cases are self-limited acute hepatitis (AH), some develop into severe forms of hepatitis (1). In fact, in the past several years, there has been an increase in the numbers of patients with sporadic hepatitis A, especially the more severe kind, visiting our hospital. Our analysis of the possible factors responsible for the disease severity in our patients revealed no significant differences in terms of background including age, suggesting that viral factors might be involved in determining the severity of the disease (2, 3).

Hepatitis A virus (HAV) is the sole member of the hepatovirus genus and a member of the Picornavirus family. Virological studies have revealed that HAV is a positive-strand RNA virus comprising approximately 7500 nucleotides and containing a 5′ nontranslated region (NTR), a single long open reading frame encoding a large polyprotein and a 3′NTR. A large polyprotein is cleaved by the viral protease to produce the P1, P2 and P3 regions. The P1 region encodes four structural proteins – VP4, VP2, VP3 and VP1. The P2 and P3 regions encode nonstructural proteins 2A, 2B and 2C, and 3A, 3B, 3C and 3D respectively (4). As far as is known, nonstructural protein 2A participates in virion morphogenesis (5). 2B and 2C play important roles in the replication of viral RNA. 2C is a multifunctional protein and is considered to have helicase and NTPase activities. 2C or 2BC have membrane- and RNA-binding properties (6). 3B is considered to be a genome-linked viral protein (Vpg), 3A a pre-Vpg, 3C a viral protease and 3D an RNA-dependent RNA polymerase.

It was reported that the strains adapted to cell culture systems have mutations in 5′NTR and the P2 region of HAV (7, 8). Zhang *et al.* (9) reported that rapidly replicating, cytopathic variants of HAV isolated from cultured cells required mutations within 5′NTR, 2B and 2C, and these mutations acted cooperatively. Raychaudhuri *et al.* (10) reported that the simian virus 2C gene could confer the phenotype of virulence to an otherwise attenuated virus, and clusters of residues near both ends of the 2C protein were required for virulence using chimeras between human and simian strains of hepatitis A virus in tamarins.

Despite advances in the understanding of HAV, a correlation between the HAV genome and the clinical status of hepatitis A has not been established. Durst *et al.* (11) reported a cluster of fulminant hepatitis A, in which the severity of the infection in three siblings was related to the virulence of HAV. To examine the possibility of differences in hepatitis A viruses in terms of the different categories of hepatitis, we have analysed the viral genomes in sera from hepatitis A patients with a variety of clinicopathological features and reported the associations between some viral regions and clinical severities (3, 12–18).

When analysing the viral genome, rather than focusing on one specific region, perhaps several portions of the HAV genome should be investigated. In the present study, we examined the clinicopathological features of hepatitis A and possible correlations with variations in the three regions of 5′NTR, 2B and 2C of the HAV genome, whose mutations have previously been shown to be important for enhanced replication and virulence in cell culture systems and simians, in the same patients using phylogenetic analysis.

Materials and methods

Patients

Serum samples from 25 patients with hepatitis A in Japan were collected between 1986 and 1999 and stored at − 20 °C until analysis. Informed consent was obtained from the patients or appropriate family members. These patients were diagnosed based on the positivity of the IgM antibody to HAV (IgM anti-HAV) in conjunction with compatible symptoms and laboratory findings.

Among the patients seven had fulminant hepatitis (FH), five had severe acute hepatitis (AHs) and 13 had self-limited AH. Patients with a prothrombin time < 40% of control were defined as AHs, and those with hepatic encephalopathy as FH. Patients with significant increases in serum blood urea nitrogen and creatinine (more than three times the upper level of the normal range) were judged to be undergoing acute renal failure. The patients were also investigated for histories of recent exposure to drugs and chemical agents as well as heavy alcohol consumption (> 50 g/day for > 5 years).

None of the patients had clinical or laboratory evidence of acquired immune deficiency syndrome.

Serological markers

IgM antibody to HBc(IgM anti-HBc), HBsAg and second-generation antibody to hepatitis C virus (HCV) were examined in all cases. IgM anti-HAV, IgM anti-HBc and HBsAg were measured by commercial radioimmunoassay kits (Abbott Laboratories, Chicago, IL, USA); second-generation HCV antibody was measured by the enzyme immunoassay kit (Ortho Diagnostics, Tokyo, Japan). In the FH and AHs patients, HCV RNA, IgM antibody to Epstein–Barr virus (IgM anti-EBV), IgM antibody to herpes simplex virus (IgM anti-HSV), IgM antibody to cytomegalovirus (IgM anti-CMV), anti-smooth muscle antibody, liver kidney microsomal antibody-1 and anti-mitochondrial antibody were also examined. HCV RNA was measured by nested reverse transcriptase-polymerase chain reaction (RT-PCR) as described by the authors (19). IgM anti-EBV, IgM anti-CMV and IgM anti-HSV were examined by enzyme-linked immunosorbent assays. Anti-nuclear antibody, anti-smooth muscle antibody, anti-mitochondrial antibody and anti-liver kidney microsomal-1 antibody were examined by the fluorescent antibody method.

Quantification of hepatitis A virus RNA by real-time reverse transcriptase-polymerase chain reaction

Serum viral RNA was extracted by the High Pure Viral RNA Kit (Roche Diagnostics GmbH, Mannheim, Germany). RT-PCR was carried out with a Hepatitis A Virus Quantification Kit (Roche Diagnostics) according to the manufacturer's instructions. Twenty microliters of the PCR mixture contained 15 μl of master mix from the kit and 5 μl of template RNA. The standards of HAV RNA are supplied with this kit. All reactions were performed in a LightCycler (Roche Diagnostics). The C_T values from clinical samples were plotted on the standard curve, and the number of copies wes calculated automatically. This method has a dynamic range of HAV RNA quantification between 0.5 and 5×10^6 copies/μl.

Amplification of serum hepatitis A virus RNA and direct sequencing

Hepatitis A virus RNA was examined by nested RT-PCR and direct sequencing as described previously (14, 17, 18).

Nucleotide sequence accession numbers

The nucleotide sequence data reported herein appear in DDBJ/EMBL/GenBank nucleotide sequence databases with the following accession numbers:

5′NTR

AB045327 for A1, AB045336 for A5, AB045330 for A204, AB045331 for A205, AB045332 for A206, AB045334 for A414, AB045338 for A601, AB045342 for A159, AB045344 for A160, AB045345 for A161, AB045350 for A302, AB045353 for A811, AB045672 for A7, AB045692

for A9, AB045568 for A20, AB045671 for A68, AB045680 for A75, AB045681 for A77, AB045366 for A162, AB045572 for A303, AB045646 for A304, AB045648 for A306, AB045649 for A307, AB045678 for A712 and AB045679 for A713.

2B

AB047652 for A1, AB047671 for A5, AB047660 for A204, AB047661 for A205, AB047662 for A206, AB047669 for A414, AB047673 for A601, AB047654 for A159, AB047655 for A160, AB047656 for A161, AB047663 for A302, AB047680 for A811, AB047675 for A7, AB047681 for A9, AB047658 for A20, AB047674 for A68, AB047678 for A75, AB047679 for A77, AB047657 for A162, AB047664 for A303, AB047665 for A304, AB047666 for A306, AB047667 for A307, AB047676 for A712 and AB047677 for A713.

2C

AB082174 for A1, AB082130 for A5, AB0821323 for A204, AB082133 for A205, AB082134 for A206, A082135 for A414, AB082137 for A601, AB082139 for A159, AB082140 for A160, AB082141 for A161, AB082145 for A302, AB082147 for A811, AB082148 for A7, AB082149 for A9, AB082150 for A20, AB082154 for A68, AB082155 for A75, AB082156 for A77, AB082160 for A162, AB082165 for A303, AB082166 for A304, AB082167 for A306, AB082168 for A307, AB082171 for A712 and AB082172 for A713.

Phylogenetic analysis

To determine the heterogeneity of the viral sequences obtained from the 25 patients, a phylogenetic tree was constructed by the neighbour-joining method. To confirm the reliability of the phylogenetic tree, bootstrap resampling tests were performed 1000 times. These analyses were conducted using a computer program, GENETYX-MAC version 10.1 (Software Development, Tokyo, Japan).

Statistical analysis

Differences in proportions among the groups were compared by Fisher's exact probability test, Student's *t*-test and Welch's *t*-test (DA STATS version 1.0, Nagata O, Tokyo, Japan).

Results

Clinicopathological characteristics of the patients

The characteristics of the 25 patients with hepatitis A analysed for HAV 5'NTR, 2B and 2C at admission are summarized in Table 1. None of the cases was associated with an epidemic.

Differences in the mean age, sex and presence of chronic liver disease among FH, AHs and AH, and between FH+AHs and AH, were not statistically significant. Serum was sampled 2–17 days after clinical onset. The mean ALT level was higher in AHs than that in AH ($P = 0.002$), and in FH+AHs than that in AH ($P = 0.003$). The mean prothrombin time was prolonged in FH compared with AHs ($P = 0.002$), FH compared with AH ($P < 0.001$), AHs compared with AH ($P < 0.001$) and FH+AHs compared with AH ($P < 0.001$). The mean total bilirubin level was higher in FH than that in AHs ($P = 0.049$).

Table 1. Characteristics of patients

	FH	AHs	AH
n	7	5	13
CLD	1†	1†	3†
Recovery/death	3/4‡	5/0‡	13/0‡
Sex (M/F)	3/4†	5/0†	7/6†
Age*	44.1 ± 13.5†	36.8 ± 12.9†	39.5 ± 9.1†
PT (%)*	16 ± 7§	34 ± 8§	63 ± 20§
ALT (IU/L)*	6337 ± 3838¶	6165 ± 1718¶	2873 ± 1733¶
T-Bil (mg/dl)*	9.4 ± 7.6‖	2.3 ± 0.8‖	5.0 ± 2.3‖

*Mean ± SD.

†Statistically not significant.

‡Statistically significant between FH and AH ($P = 0.007$) by Fisher's exact probability test.

§Statistically significant between FH and AHs ($P = 0.002$) by Student's *t*-test, FH and AH ($P < 0.001$) by Welch's *t*-test, and AHs and AH ($P < 0.001$) by Welch's *t*-test.

¶Statistically significant between AHs and AH ($P = 0.002$) by Student's *t*-test.

‖Statistically significant between AHs and FH ($P = 0.049$) and AHs and AH ($P = 0.002$) by Welch's *t*-test.

AH, acute hepatitis; AHs, severe acute hepatitis; ALT, alanine aminotransferase; CLD, chronic liver disease; FH, fulminant hepatitis; PT, prothrombin time; T-Bil, total bilirubin.

Four of seven patients with FH died of hepatic failure, and all patients with AHs and AH recovered ($P = 0.007$). All seven FH cases needed artificial liver support (plasma exchange and haemodiafiltration). Four (16%) patients – two (28%) with FH and two (15%) with AH – had acute renal failure and were treated by haemodiafiltration.

Two patients with AH were positive for HBsAg and antibody to HBe, and one patient with AH was positive for anti-nuclear antibody, but they showed a typical hepatitis A course. IgM anti-EBV, IgM anti-HSV, IgM anti-CMV, anti-nuclear antibody, anti-smooth muscle antibody, liver kidney microsomal antibody-1 and anti-mitochondrial antibody were negative in all examined cases of FH and AHs. One FH patient and one AHs patient had histories of heavy alcohol consumption. One male patient with AH was homosexual.

Histological examination was performed in all seven FH cases, two of five AHs cases and seven of 13 AH cases in the convalescent phase or postmortem. In the FH cases, liver histology revealed massive necrosis in three patients and submassive necrosis in one. Liver histology in the two patients with histories of heavy alcohol consumption showed pericellular fibrosis, consistent with alcoholic liver disease. The histological findings of the other cases showed AH to be in a residual phase or subsiding.

Phylogenetic analysis

The results of phylogenetic analysis are shown in Figures 1 and 2. Four FH (A204, A601, A414 and A1) and two AHs (A160 and A159) were located in the near parts of the phylogenetic trees (Fig. 2).

The clinical backgrounds, and the biochemical and viral characteristics are shown in Table 2. As described above, none of them were associated with an epidemic. Two of the FH patients died and the others recovered. HAV RNA was quantified by real-time RT-PCR in five of these six patients. Our other recent study of HAV RNA quantification revealed that the mean viral load in > 60 AH at admission was 2.75 ± 1.55 log copies/ml (20), and so these five patients had comparatively higher viral loads (4.35 ± 0.81 log copies/ml) ($P = 0.03$). The HAV genotype was IA in all patients, similar to the majority of Japanese patients in general.

Discussion

Although the severity of hepatitis A varies, it is not clear why it is more severe in some patients than that in others. It is thought that disease severity may be dependent on certain characteristics of the individual patients. It has been reported that ageing and underlying chronic liver disease could be factors that increase hepatitis A severity (21). Vento *et al.* (22) reported that patients with chronic hepatitis C had a substantial risk of FH and death associated with HAV superinfection.

During an urban epidemic in the US, it was described that hepatitis A caused serious illness and death and that complications were more frequent in patients 40 years of age and older, but that young healthy persons were also at risk for severe complications (23). A cluster of fulminant hepatitis A was reported, relating the severity of the infection in three siblings to the virulence of HAV, as the patients were all healthy before the infection and their illness followed a similar course (11).

In the past several years, increasing numbers of patients with sporadic hepatitis A, especially the more severe forms, have visited our hospital, but our analysis of factors possibly contributing to the severity of the disease failed to reveal any significant differences in patient characteristics including age (2, 3), suggesting that viral factors might determine the severity of the disease. To identify possible differences in hepatitis A viruses for different types of hepatitis, we analysed the HAV genome in sera from hepatitis A patients with various clinicopathological features. Our analysis of whole HAV genomes from three cases of FH and three cases of AH indicated possible associations between the severity of hepatitis A and the nucleotide substitutions in 5′NTR and the amino acid (aa) substitutions in 2B, although there were no unique nucleotide or aa substitutions. On the other hand, it was reported that mutations in 5′NTR, 2B and 2C of HAV were associated with cytopathic variants in cultured cells, and virulence in tamarins, as described above (9, 10). These various observations led us to analyse these three regions of HAV in greater numbers of clinical samples (14, 17, 18).

In our analysis of 5′NTR, FH and AHs patients had fewer nucleotide substitutions than AH in the central part of 5′NTR ($P < 0.001$) (14). Several regions of 5′NTR, including the pyrimidine-rich tract and internal ribosomal entry site, have been examined for possible correlations with replication of HAV RNA *in vitro*, and it has been reported that HAV strains adapted to cell culture systems have mutations in 5′NTR and the P2 region (8), and mutations in 5′NTR significantly enhanced growth of the virus in a cell culture system (24). Thus, nucleotide variations in 5′NTR may influence replication of the virus and thereby affect virulence.

In 2B, there seemed to be more mutations in the strains obtained from FH and AHs patients than in those obtained from AH patients in the central part (18). On the basis of cell culture studies, substitutions in the sequence of 2B protein have been suggested to be associated with the replication capability of the virus. One nucleotide substitution at nt 3889 in 2B, which changed Ala to Val in 2B-216, is responsible for differences in the growth rate of the virus along with the nucleotide substitutions in 2C and/or 5′NTR (25, 26). A substitution at the same nt 3889 appeared from the early stage of replication enhancement in cultured cells, and several HAV strains showed a cytopathic effect (8). An Ala-to-Val substitution in 2B-216 was not observed in our study.

In 2C, FH patients had fewer aa substitutions than AH patients ($P < 0.05$) (17). This indicates that viruses with fewer aa substitutions in 2C may be more virulent in comparison with strains with more aa substitutions. 2C is a multifunctional protein and is involved in replication of the viral genome. Analysis of the primary aa sequence of 2C shows homology with a family of proteins that contains a nucleoside triphosphate (NTP)-binding motif. This motif consists of elements 'A' and 'B'. The residues mutated within the conserved A and B sites of the NTP-binding motif are critical in RNA replication and virus proliferation (27). Elements A and B were conserved in all patients except one of FH. 2C is also suggested to be involved in the rearrangement of cellular membranes (28). The simian HAV 2C gene was reported to be required for virulence in tamarins (10). Thus, subtle substitutions in 2C might influence the replication capability of the virus and thereby affect virulence. We could not find specific nucleotide or aa substitutions in any of the regions.

In the present study, patients with FH had fewer nt substitutions in 5′NTR, and had a tendency to have more aa substitutions in 2B, and fewer aa substitutions in 2C, than patients with AH, and four FH and two AHs were located in the near parts of the phylogenetic trees, indicating the association between severity of hepatitis A and genomic variations in 5′NTR, 2B and 2C of HAV. In these patients, HAV load was higher than that of AH

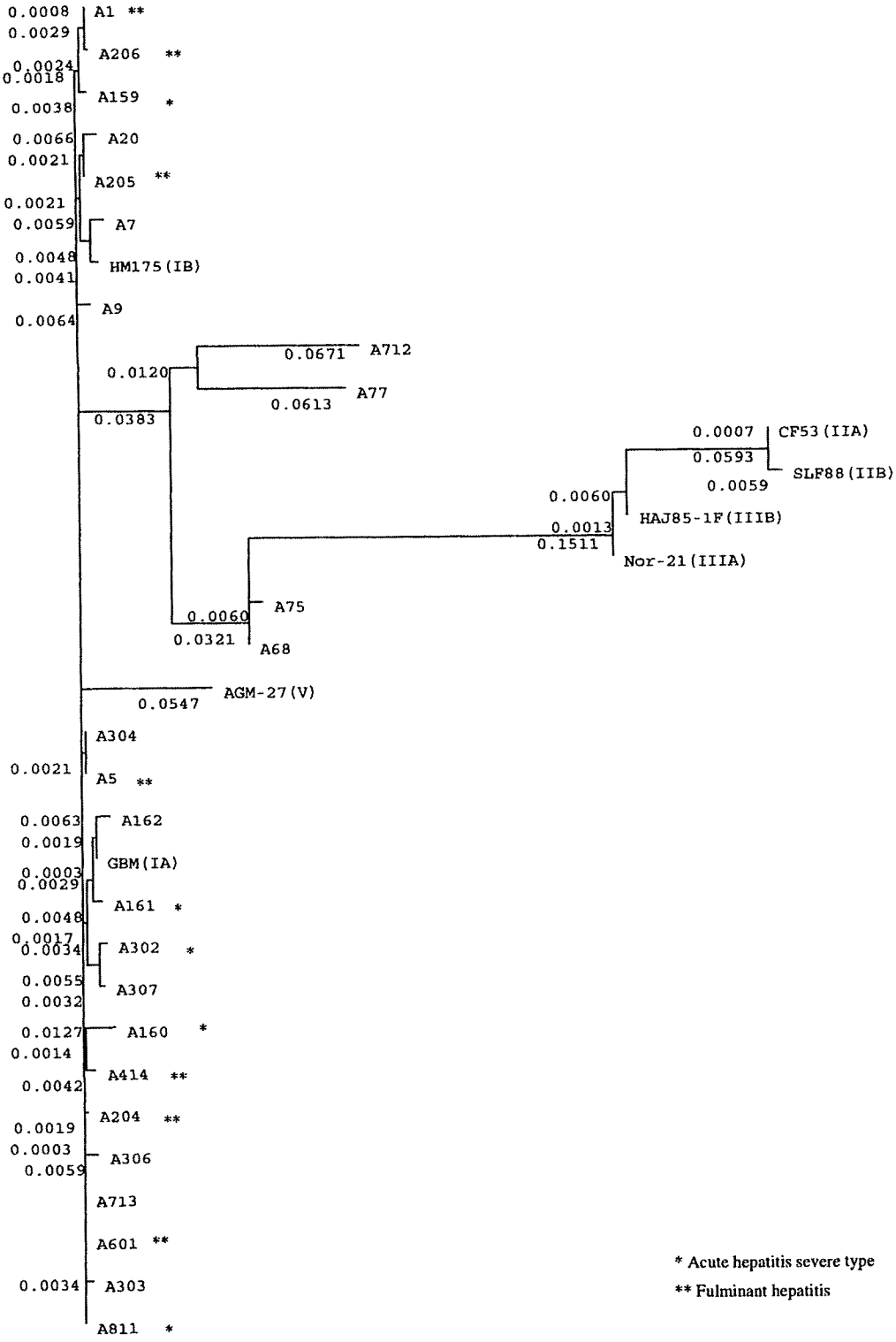

Fig. 1. Genetic relatedness between individual hepatitis A virus (HAV) strains between nucleotides 200 and 500 of the 5′ nontranslated region recovered from 25 patients and HAV reference strains GBM (subgenotype IA), HM175 (subgenotype IB), CF53 (subgenotype IIA), SLF88 (subgenotype IIB), Nor-21 (subgenotype IIIA), HAJ85-1F (subgenotype IIIB) and AGM27 (genotype V). Numbers beside the phylogenetic roots are the results of bootstrap analyses.

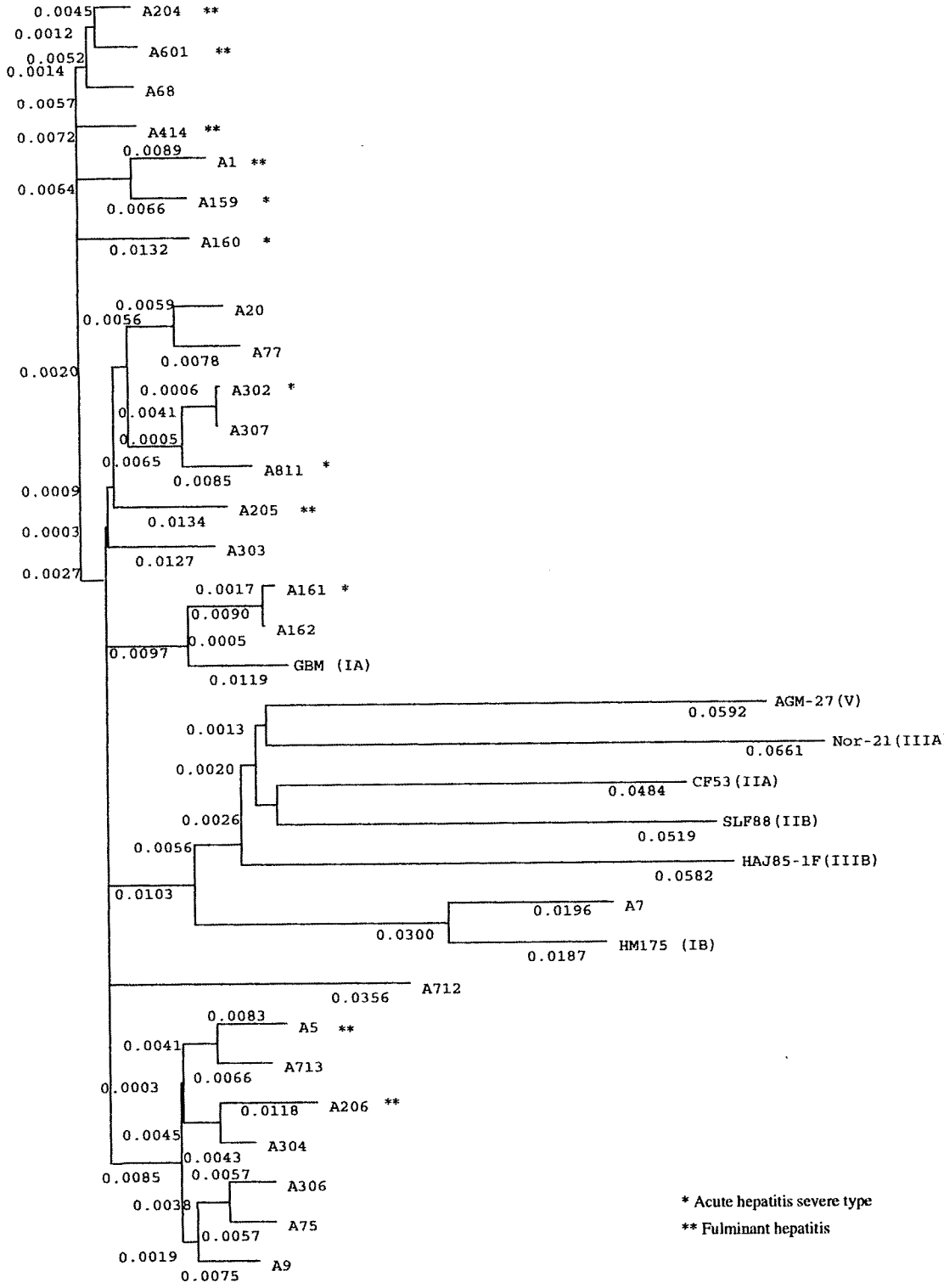

Fig. 2. Genetic relatedness between individual hepatitis A virus (HAV) of entire 2B and 2C recovered from 25 patients and HAV reference strains GBM (subgenotype IA), HM175 (subgenotype IB), CF53 (subgenotype IIA), SLF88 (subgenotype IIB), Nor-21 (subgenotype IIIA), HAJ85-1F (subgenotype IIIB) and AGM27 (genotype V). Numbers beside the phylogenetic roots are the results of bootstrap analyses.